



Publication Year	2008
Acceptance in OA @INAF	2023-01-24T13:12:07Z
Title	Detection of C3O in the low-mass protostar Elias 18
Authors	PALUMBO, Maria Elisabetta; LETO, PAOLO; Siringo, C.; TRIGILIO, CORRADO
DOI	10.1086/591017
Handle	http://hdl.handle.net/20.500.12386/33036
Journal	THE ASTROPHYSICAL JOURNAL
Number	685

DETECTION OF C₃O IN THE LOW-MASS PROTOSTAR ELIAS 18

M. E. PALUMBO

INAF-Osservatorio Astrofisico di Catania, I-95123 Catania, Italy; mepalumbo@oact.inaf.it

P. LETO

INAF-Istituto di Radioastronomia, Sezione Noto, Italy

C. SIRINGO

Università degli Studi di Catania, Dipartimento di Fisica ed Astronomia, Catania, Italy

AND

C. TRIGILIO

INAF-Osservatorio Astrofisico di Catania, I-95123 Catania, Italy

Received 2008 February 15; accepted 2008 June 6

ABSTRACT

We have performed new laboratory experiments which gave us the possibility to obtain an estimate of the amount of carbon chain oxides (namely C₃O₂, C₂O, and C₃O) formed after irradiation (with 200 keV protons) of pure CO ice, at 16 K. The analysis of laboratory data indicates that in dense molecular clouds, when high CO depletion occurs, an amount of carbon chain oxides as high as $(2-3) \times 10^{-3}$ with respect to gas phase carbon monoxide can be formed after ion irradiation of icy grain mantles. Then we searched for gas phase C₂O and C₃O toward 10 low-mass young stellar objects. Among these we detected the C₃O line at 38486.891 MHz toward the low-mass protostar Elias 18. On the basis of the laboratory results we suggest that in dense molecular clouds gas phase carbon chain oxides are formed in the solid phase after cosmic ion irradiation of CO-rich icy mantles and released to the gas phase after desorption of icy mantles. We expect that the Atacama Large Millimeter Array (ALMA), thanks to its high sensitivity and resolution, will increase the number of carbon chain oxides detected in dense molecular clouds.

Subject headings: astrochemistry — ISM: individual (Elias 18) — ISM: molecules — methods: laboratory

1. INTRODUCTION

One of the main open questions in astrochemistry regards the relation between solid phase and gas phase chemistry in dense molecular clouds. In fact, in these regions ice mantles form on silicatic and carbonaceous grains after both direct freeze out of gas phase species and grain surface reactions. The presence of icy grain mantles is indirectly deduced from depletion of gas phase species and directly observed in the infrared from absorption features, attributed to vibrational modes of solid phase molecules, superposed to the background stellar spectrum. Icy grain mantles have been detected both in quiescent regions and in star-forming regions. In both environments these suffer from energetic processing due to cosmic ions and UV photons. Ion and UV irradiation cause a modification of the structure and of the chemical composition of grain mantles, that is, the formation of molecular species not present in the original ice. After desorption of icy mantles molecular species are released to the gas phase, which could be enriched by species formed in the solid phase.

Previous laboratory experiments have shown that carbon chain oxides (e.g., C₂O, C₃O, C₃O₂, C₄O, C₅O₂, C₇O₂) are formed after ion irradiation and UV photolysis of CO-rich ice mixtures (e.g., Strazzulla et al. 1997; Gerakines & Moore 2001; Trottier & Brooks 2004; Loeffler et al. 2005) along with carbon dioxide (CO₂), which is the most abundant molecule formed (e.g., Gerakines et al. 1996; Loeffler et al. 2005).

Carbon chain oxides, namely dicarbon monoxide (C₂O) and tricarbon monoxide (C₃O), have been detected in the molecular cloud TMC-1 toward the cyanopolyne peak (hereafter TMC-1CP), and it has been estimated that fractional abundance of

C₂O is about 6×10^{-11} and that of C₃O is about 1.4×10^{-10} . These abundances have been explained by ion-molecule gas phase reactions (Matthews et al. 1984; Brown et al. 1985; Ohishi et al. 1991; Kaifu et al. 2004). C₃O has also been extensively searched for (Matthews et al. 1984; Brown et al. 1985) toward other objects, some of which are rich molecular-line sources and which together encompass a wide range of physical conditions. However, C₃O was not detected in these regions and only upper limits have been estimated. Recently, C₃O (Tenenbaum et al. 2006) as well as other O-bearing species, such as H₂O (Melnick et al. 2001; Hasegawa et al. 2006), OH (Ford et al. 2003), and H₂CO (Ford et al. 2004), have been detected toward the carbon star IRC+10216. This is an asymptotic giant branch star. O-bearing molecules are not expected in carbon stars since the bulk of available oxygen is contained in CO. In order to explain these observations it has been suggested that the increase in the star luminosity is causing the evaporation of orbiting icy bodies (Melnick et al. 2001). Alternatively, it has been suggested that gas phase oxygen-rich chemistry is occurring in the outer shell of the star (Tenenbaum et al. 2006).

Here we discuss new laboratory experiments which confirm the formation of carbon chain oxides after ion irradiation of CO ice at low temperature and give us the opportunity to obtain a quantitative estimate of the amount of carbon chain oxides formed with respect to initial carbon monoxide (§ 2). We present the new detection of the C₃O line at 38486.891 MHz toward the low-mass protostar Elias 18, and we confirm the detection of the same line toward TMC-1CP, as already reported by Kaifu et al. (2004) (§ 3). On the basis of our laboratory results we suggest that gas phase carbon chain oxides in dense molecular clouds are actually formed in the solid phase after ion irradiation of CO-rich

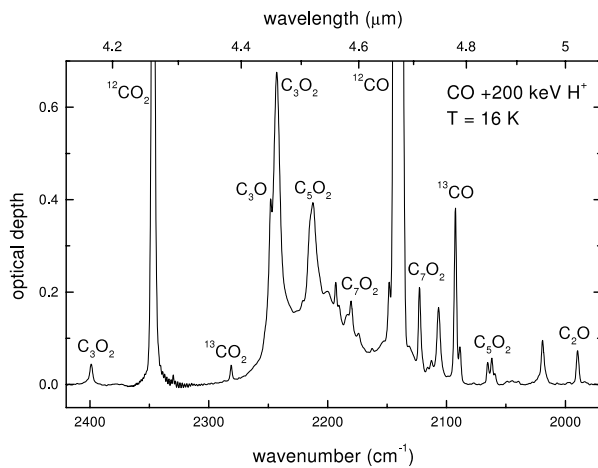


FIG. 1.— Infrared transmission spectrum, in optical depth scale, of CO ice after ion irradiation with 200 keV H^+ (fluence = 1.25×10^{14} ions cm^{-2}) at 16 K. Labels indicate main species present after irradiation.

icy grain mantles and released to the gas phase after desorption of icy mantles (§ 4).

2. EXPERIMENTAL RESULTS

Experiments have been performed in the Laboratory for Experimental Astrophysics (INAF-Catania Astrophysical Observatory, Italy). A detailed description of the experimental setup can be found elsewhere (e.g., Strazzulla et al. 2001; Baratta et al. 2002; Palumbo et al. 2004). CO icy samples were prepared on a cold substrate (16 K) in a vacuum chamber ($P = 10^{-7}$ mbar) and then irradiated with 200 keV H^+ ions. Mid-IR transmission spectra ($2.5\text{--}25 \mu m$; $4000\text{--}400 \text{ cm}^{-1}$) were taken before, during,

TABLE 1
MOST INTENSE FEATURES DETECTED AFTER IRRADIATION
WITH 200 keV H^+ IONS OF CO ICE AT 16 K
AND THEIR IDENTIFICATION.

Band Position (cm^{-1})	Identification
3706.....	CO ₂
3601.....	CO ₂
3069.....	C ₃ O ₂
2398.....	C ₃ O ₂
2340.....	CO ₂
2329.....	C ¹⁶ O ¹⁸ O
2280.....	¹³ CO ₂
2247.....	C ₃ O
2242.....	C ₃ O ₂
2211.....	C ₃ O ₂
2192.....	OCC ¹³ CO
2179.....	C ₇ O ₂
2140.....	CO
2122.....	C ₇ O ₂
2112.....	C ¹⁷ O
2105.....	...
2092.....	¹³ CO
2088.....	C ¹⁸ O
2064.....	...
2061.....	C ₅ O ₂
2018.....	...
1989.....	C ₂ O
1924.....	...
1918.....	C ₄ O
1042.....	O ₃

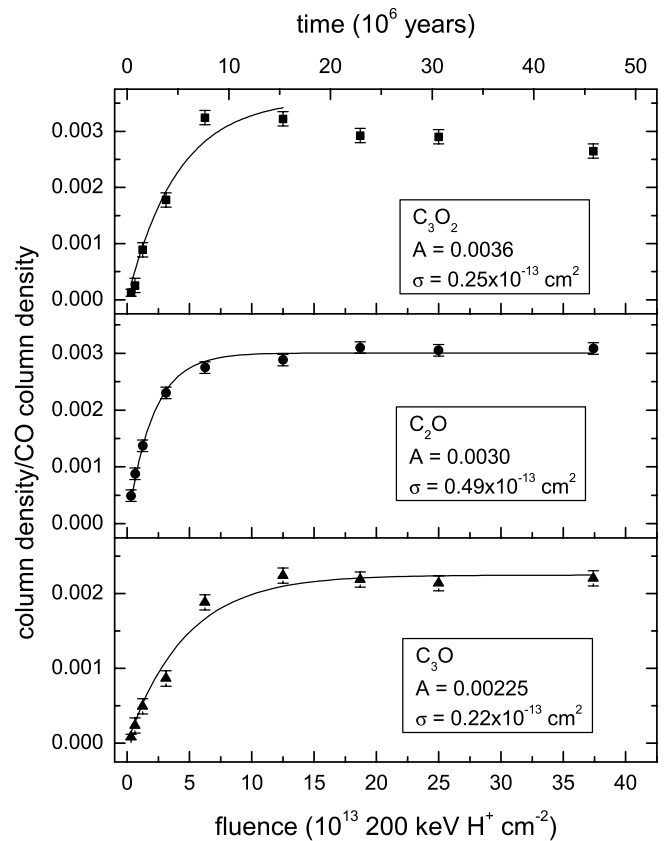


FIG. 2.— Column densities of C_3O_2 , C_2O , and C_3O with respect to column density of initial CO as a function of fluence after ion irradiation of pure CO at 16 K with 200 keV H^+ . The top x -axis indicates the time (in 10^6 yr) which would be necessary to obtain in dense molecular clouds the same effects observed in laboratory. The experimental data have been fitted with an exponential curve (solid lines) and the fit parameters for each species are reported.

and after irradiation. Different CO icy samples were irradiated and the highest ion fluence was 1.5×10^{15} ions cm^{-2} . Figure 1 shows the spectrum of pure carbon monoxide in the $2450\text{--}1950 \text{ cm}^{-1}$ ($4.08\text{--}5.1 \mu m$) spectral range at 16 K after irradiation with 200 keV H^+ ions (fluence equal to 1.25×10^{14} ions cm^{-2}). It

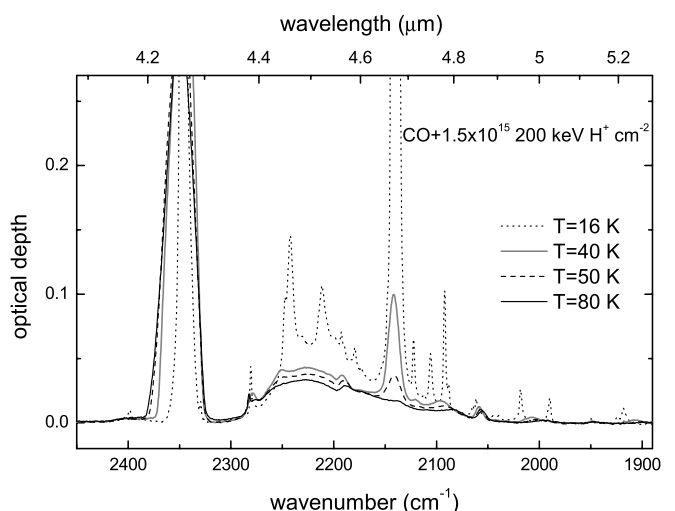


FIG. 3.— Infrared transmission spectra, in optical depth scale, of CO ice after ion irradiation with 200 keV H^+ (fluence = 1.5×10^{15} ions cm^{-2}). Spectra taken at 16 K and after warm up are shown.

TABLE 2
LOW-MASS YOUNG STELLAR OBJECTS OBSERVED

Object ^a	Region	α (J2000.0)	δ (J2000.0)
TMC-1CP.....	Taurus	04 41 45.9	25 41 27
TMC1-A.....	Taurus	04 39 35.0	25 41 47
Elias 18.....	Taurus	04 39 55.7	25 45 02
L1551 IRS5.....	Taurus	04 31 33.9	18 08 08
L1489IR.....	Taurus	04 04 43.1	26 18 58
Elias 29 (WL15).....	Ophiuchus	16 27 09.3	-24 37 21
Elias 32 (VS18).....	Ophiuchus	16 27 28.5	-24 27 17
WL5.....	Ophiuchus	16 27 18.0	-24 28 52
CK1 (SVS20).....	Serpens	18 29 57.5	01 14 07
SVS4.....	Serpens	18 29 57.8	01 12 48

NOTE.—Units of right ascension are hours, minutes, and seconds, and units of declination are degrees, arcminutes, and arcseconds.

^a Other ID is given in parentheses.

is evident that after irradiation several absorption features are present which indicate the formation of molecular species not present in the original ice sample. In Figure 1 the intense CO band at about 2139 cm⁻¹ (4.67 μ m) and the CO₂ band at about 2343 cm⁻¹ (4.27 μ m) are out of scale. Main carbon chain oxides bands formed after irradiation are labeled. In Table 1 the peak position of most intense bands is reported along with their identification, which is based also on the results presented by Trotter & Brooks (2004). A few features listed in Table 1 still remain unidentified and further laboratory experiments will be necessary for their identification.

Figure 2 shows the column density of carbon suboxide (C₃O₂), tricarbon monoxide (C₃O), and dicarbon monoxide (C₂O) with respect to initial carbon monoxide as a function of ion fluence after irradiation of CO ice at 16 K. Column density of C₃O₂ was obtained from the band at 2398 cm⁻¹ using the integrated absorbance value of 0.8 $\times 10^{-17}$ cm molecule⁻¹ given by Gerakines & Moore (2001). The column density of C₃O and C₂O have been obtained from the bands at 2247 and 1989 cm⁻¹, respectively. We note that the 2247 cm⁻¹ band is superposed to the broader band at about 2242 cm⁻¹ due to C₃O₂. In order to estimate the integrated intensity (area) of this band we considered a linear baseline between 2246.7 and 2249.6 cm⁻¹. Given that the integrated absorbance of bands due to C₃O and C₂O has not been measured we assumed a value of 1 $\times 10^{-17}$ cm molecule⁻¹ for both bands. In

fact, this value is close to the average value measured for the absorption bands of many molecules (e.g., Mulas et al. 1998; Kerkhof et al. 1999; Bennett et al. 2004). The initial column density of carbon monoxide (the 2140 cm⁻¹ band being saturated) has been measured from the interference curve given by a He-Ne laser beam reflected both by the vacuum-film and film-substrate interfaces (e.g., Baratta & Palumbo 1998) during accretion of the ice sample. An ice density equal to 0.8 g cm⁻³ (Loeffler et al. 2005) was used to obtain the column density value. The ratio of the column density of each species relative to the initial CO column density as a function of ion fluence has been fitted with the exponential curve $y = A(1 - e^{-\sigma\Phi})$, where Φ is the ion fluence (ions cm⁻²), σ is the process cross section (cm²), and A is the asymptotic value of the column density ratio. The σ and A values obtained for each species are reported in Figure 2. In the case of C₃O₂, only data points obtained at ion fluence lower than 1.25 $\times 10^{14}$ ions cm⁻² have been considered in the fitting procedure. In fact, we noted that at higher fluence the column density of carbon suboxide decreases, indicating that this species is destroyed after further irradiation. This also occurs with dicarbon monoxide and tricarbon monoxide at fluences higher than those given in Figure 2. This effect has in fact already been observed for species formed after ion irradiation of other ice samples (e.g., Baratta et al. 2002). As discussed in detail in § 4, the top x -axis in Figure 2 gives an estimation of the time (in 10⁶ yr) necessary to obtain on interstellar ices the same effects observed in laboratory. After irradiation was completed ice samples were warmed up and spectra were taken at 25, 40, 50, 60, 70, and 80 K. The spectrum at 25 K is almost indistinguishable from that taken at 16 K. Spectra taken at 16, 40, 50, and 80 K are shown in Figure 3. It is evident that the intensity of absorption bands due to CO and carbon chain oxides rapidly decreases after warm up and that these are not detectable at about 80 K. On the other hand, the bands due to carbon dioxide are present in the spectra at higher temperatures. This indicates that volatile species such as CO and carbon chain oxides sublimate. Finally, it is worth mentioning that carbon chain oxides are not formed after ion irradiation of O-rich ice samples such as CO₂:CO and H₂O:CO mixtures (Strazzulla et al. 1997).

3. OBSERVATIONS

Radio observations were performed on 2006 September 6–12 with the 32 m radiotelescope in Noto (Italy). Sources observed

TABLE 3
OBSERVATION LOG AND RMS MEASURED

SOURCE	CCO $\nu = 22258.181$ MHz $J_N = 2_1-1_0$		CCO $\nu = 45826.706$ MHz $J_N = 3_2-2_1$		C ₃ O $\nu = 38486.891$ MHz $J = 4-3$	
	Int. Time	rms	Int. Time	rms	Int. Time	rms
	(minutes)	(K)	(minutes)	(K)	(minutes)	(K)
TMC-1CP.....	300	0.008	140	0.011	380	0.005
TMC-1A.....	160	0.010
Elias 18.....	180	0.010	140	0.008	200	0.007
L1551 IRS5.....	300	0.007	150	0.009	300	0.007
L1489IR.....	300	0.008	220	0.001	240	0.008
Elias 29.....	90	0.016	90	0.019	200	0.008
Elias 32.....	90	0.016	90	0.022	160	0.011
WL5.....	90	0.018	80	0.025	160	0.009
...
CK1.....	120	0.013	120	0.014	230	0.006
SVS4-4.....	200	0.011	120	0.015	160	0.008

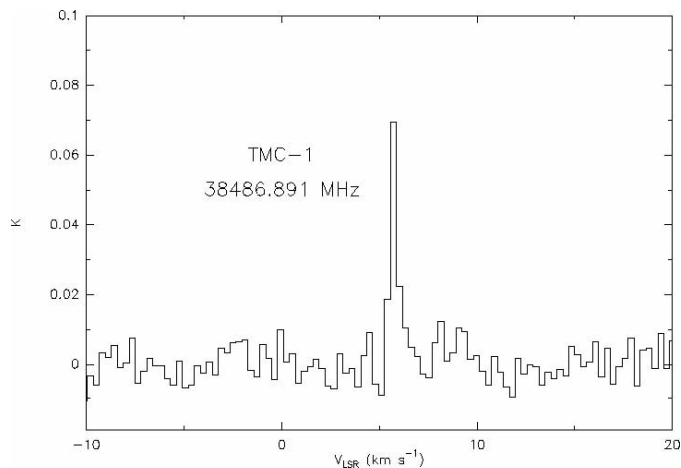


FIG. 4.—C₃O line at 38486.891 MHz detected toward TMC-1CP.

are listed in Table 2. The telescope has an active surface system that compensates the gravitational deformation of the primary mirror, making observations at high frequencies also possible. This new antenna setup, together with the favorable weather conditions, allow it to operate with good performance at high frequencies.

The observations were carried out using the 22 GHz and the new 43 GHz (that can be tuned in the 38–47 GHz range) receivers. The beam size of the telescope (HPBW) was about 115'' at 22 GHz and 54'' at 43 GHz; the system noise temperature (including atmospheric noise and antenna ohmic losses) is about 90–120 K at zenith, depending on weather conditions. The aperture efficiency of the telescope was about 0.28 at 43 GHz and 0.44 at 22 GHz. A duty cycle of 5 minutes integration on source and 5 minutes off source was used. Total integration time for each source is reported in Table 3.

The spectra were acquired with the ARCOS autocorrelator (Comoretto et al. 1990) in beam switch mode; two spectra, one for each polarization, were acquired simultaneously. Each spectrum has a bandwidth of 20 MHz, with a spectral resolution of 37 kHz, corresponding to a velocity resolution of 0.27 and 0.53 km s⁻¹ at 43 and 22 GHz, respectively. The determination of the antenna efficiency as a function of the elevation was performed by observing the flux calibrators 3C 286, 3C 123, and NGC 7027. The spectra were reduced by using the software XSpetro for the on-off difference, then CLASS software for the baseline subtraction and temperature calibration. The antenna temperature was corrected to account for the variation of the effective area of the telescope as a function of elevation. Then all spectra were averaged.

We searched for the C₂O lines at 22258.181 and 45826.706 MHz and the C₃O line at 38486.891 MHz toward the low-mass young stellar objects listed in Table 2. Our sample also includes TMC-1CP where the above lines have already been detected (Matthews et al. 1984; Brown et al. 1985; Ohishi et al. 1991; Kaifu et al. 2004). Figure 4 shows the C₃O line at 38486.891 MHz toward TMC-1CP. This detection confirms the previous results. We have not been able to confirm the detection of C₂O toward TMC-1CP as reported by Ohishi et al. (1991) and Kaifu et al. (2004), probably due to the low signal-to-noise ratio (S/N) of our measurements. Figure 5 shows the C₃O line at 38486.891 MHz toward Elias 18. The peak intensity of the line is 0.031 K (S/N = 4.4 with rms = 0.007 K). Rms values for all the sources of our sample are given in Table 3. Fitting the line profile with a Gaussian curve, we measured that the integrated intensity of the line observed toward TMC-1CP is 0.039 ± 0.008 K km s⁻¹ and is

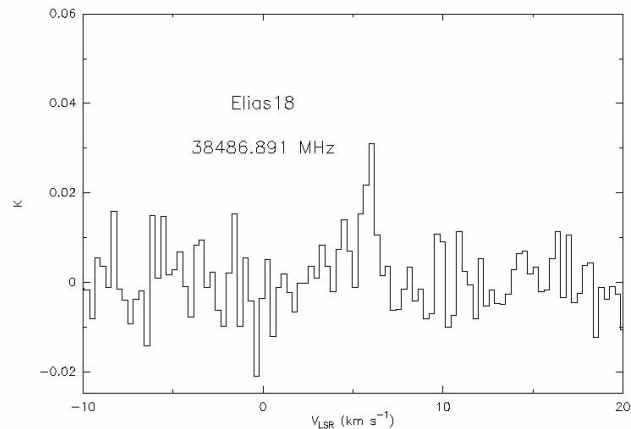


FIG. 5.—C₃O line at 38486.891 MHz detected toward Elias 18.

0.025 ± 0.005 K km s⁻¹ toward Elias 18. For the hypothesis that the source fills the antenna beam, assuming that the line is optically thin, using $T_{\text{ex}} = 20$ K, $\mu(\text{C}_3\text{O}) = 2.39$ D, and $B_0 = 4810.885$ MHz (Brown et al. 1983), and following the procedure described by Goldsmith & Langer (1999), we estimated that the C₃O column density is $(8 \pm 2) \times 10^{11}$ molecules cm⁻² toward TMC-1CP and $(5.2 \pm 1.3) \times 10^{11}$ molecules cm⁻² toward Elias 18. The value of the C₃O column density toward TMC-1CP we have found is lower than the value $[(1.4 \pm 0.4) \times 10^{12}$ molecules cm⁻²] reported by Matthews et al. (1984) and Brown et al. (1985); however, we believe that within the uncertainties of the estimation these values are comparable. Assuming $N(\text{H}_2) \simeq 1 \times 10^{22}$ molecules cm⁻² (Guelin et al. 1982), we obtain an abundance of C₃O with respect to hydrogen of about 10^{-11} .

4. DISCUSSION

Observations have shown that in dense molecular clouds the fractional abundance of carbon chain oxides (namely C₂O and C₃O) is of the order of 10^{-11} to 10^{-10} (Matthews et al. 1984; Brown et al. 1985; Ohishi et al. 1991; Kaifu et al. 2004; this work). In these regions the fractional abundance of CO is of the order of 10^{-4} and the abundance of carbon chain oxides with respect to CO is about 10^{-7} to 10^{-6} . Laboratory experiments presented here indicate that after ion irradiation of pure CO ice at 16 K the amount of carbon chain oxides formed is of the order of $(2-3) \times 10^{-3}$ with respect to initial CO (Fig. 2). In order to estimate the time necessary to obtain in dense molecular clouds the effects observed in the laboratory, we consider the approximation of effective monoenergetic 1 MeV protons and assume that in dense interstellar regions the 1 MeV proton flux is equal to 1 proton cm⁻² s⁻¹ (see Mennella et al. [2003] for a detailed discussion). However, our experimental results were obtained using 200 keV protons. Thus in order to extrapolate the laboratory results to the interstellar medium conditions we assume that they scale with the stopping power (S , energy loss per unit path length) of impinging ions. Using the TRIM code (J. F. Ziegler 2003¹), we have estimated that the stopping power ratio for protons $S(200 \text{ keV})/S(1 \text{ MeV})$ is 3.8 in the case of pure CO ice. With these hypotheses in mind we have indicated in Figure 2 a timescale axis (top x -axis), which gives an estimation of the time (in 10^6 yr) necessary to obtain the effects, observed in the

¹ Stopping and Range of Ions in Matter SRIM2003, available at <http://www.srim.org>.

laboratory, on interstellar ices. Thus if we assume high CO depletion and that the carbon chain oxides/CO column density ratio obtained in the solid phase after ion irradiation is maintained in the gas phase after desorption of icy grain mantles, then from the exponential equation used to fit the data, we find that about 10^3 yr would be necessary to form the observed column density of carbon chain oxides. As we will discuss below, this time is much shorter than the evolution timescale of dense clouds; thus the observed gas phase abundance of carbon chain oxides could be easily reached even if carbon monoxide is not completely depleted and/or only partial desorption of icy grain mantles takes place.

Toward all the young stellar objects observed in this work, the solid CO absorption band at $4.67 \mu\text{m}$ has been detected (e.g., Kerr et al. 1993; Chiar et al. 1994, 1995; Teixeira et al. 1998) along with the $3 \mu\text{m}$ band due to water ice, which is the most abundant solid phase species along these lines of sight. Recently, however, a detailed study of the solid CO band profile observed toward a large sample of low-mass embedded objects (Pontoppidan et al. 2003) has shown that typical lines of sight have 60%–90% of the solid CO in a pure or nearly pure form, suggesting that interstellar ices are best represented by a layered model rather than a mixed ice (e.g., Fraser et al. 2004). The presence of solid CO toward TMC-1CP has never been reported. In the Taurus molecular cloud a threshold extinction $A_{\text{th}} \sim 6$ mag is required for CO ice detection (Chiar et al. 1995). Gas-phase models use $A_V = 10$ mag in TMC-1 cores (e.g., Park et al. 2006), while $A_V = 32$ mag toward TMC-1A (Teixeira & Emerson 1999); thus it seems reasonable to assume that CO ice is also present along the line of sight of TMC-1CP.

Elias 18 resides in a part of the Taurus molecular cloud known as Heiles cloud 2 (HCL2) where low-mass star formation is active. It is a highly obscured object ($A_V \sim 15$ –19 mag), and it has been suggested (Tegler et al. 1995) that it is in transition between an embedded young stellar object and an exposed T Tauri star. The IR spectral energy distribution (SED) for this source is typical of a Class II or “flat-spectrum” YSO with significant optical extinction (Elias 1978). Recent observations indicate that Elias 18 has a circumstellar disk oriented close to edge-on and that most of the CO in the disk is incorporated in icy mantles on dust grains, i.e., high depletion is observed (Shuping et al. 2001). Mid-IR observations toward Elias 18 show the presence of both the solid CO and CO₂ absorption bands (e.g., Tielens et al. 1991; Chiar et al. 1995; Nummelin et al. 2001). The comparison between observations relative to solid CO and laboratory spectra indicates that different ice mixtures can equally well reproduce the observed band profile (Palumbo & Strazzulla 1993; Chiar et al. 1995, 1998). However, all the fits indicate that a comparable amount of solid CO is in the nonpolar (i.e., CO-rich) and polar (i.e., H₂O-rich) components. Among the fits obtained, it has been shown that the nonpolar component can be reproduced by the spectrum of ion-irradiated pure CO ice (and this is compatible with the hypothesis that CO-rich icy mantles are present along the line of sight in order to form carbon chain oxides) and the polar component can be reproduced by the spectrum of CO formed after ion irradiation of a H₂O : CH₃OH ice

mixture (Palumbo & Strazzulla 1993). Detection of the stretching mode band of solid CO₂ toward Elias 18 and the comparison of the observed band profile with laboratory spectra have been reported by Nummelin et al. (2001). However, as discussed by Ehrenfreund et al. (1997), Gerakines et al. (1999), and Ioppolo et al. (2008), the profile of the stretching mode band does not strongly depend on the ice mixture and cannot be used to constrain the ice composition along the line of sight.

TMC-1CP is a dense core in the TMC-1 cold dark cloud. Based on gas phase observations and chemical evolution models it has been deduced that its age is about 10^5 yr and the density is $n_{\text{H}} = 2 \times 10^4 \text{ cm}^{-3}$ (Park et al. 2006). Thus the gas would take $10^9/n_{\text{H}} = 5 \times 10^4$ yr to condense on grains (Tielens & Allamandola 1987). The presence of gas phase species implies that desorption processes, such as photodesorption, grain-grain collisions, cosmic ray induced desorption, and turbulence, compete with mantle accretion in this region (Boland & de Jong 1982; Hasegawa & Herbst 1993; Bringa & Johnson 2004).

Thus detection of C₃O toward these lines of sight is compatible with the hypothesis that this molecular species is formed in the solid phase and released to the gas phase when desorption of icy mantles takes place.

The results here discussed do not exclude carbon chain oxides from being formed after gas phase reactions in dense molecular clouds as well. Furthermore, we are aware that further observational data are necessary to confirm these results. In fact, we plan to search for carbon chain oxides toward other sources in particular hot corinos in Class 0 low-mass protostellar objects where evidence of ice mantle evaporation has been reported (Bottinelli et al. 2007).

One of the mysteries of interstellar chemistry is the mechanism regulating the balance between gas phase and solid phase species. Carbon chain oxides could be key molecules in this field, and thanks to its high sensitivity and resolution the Atacama Large Millimeter Array (ALMA) will give important results, increasing the number of detected features in a larger sample of molecular clouds.

Finally, as far as we know, the detection of C₂O and C₃O in comets has never been reported. However, comets suffer from heavy ion irradiation (Strazzulla & Johnson 1991) and CO is abundant in these objects; thus we expect that carbon chain oxides are present in comets too. In fact, a tentative detection of carbon suboxide (C₃O₂) in comet Halley has been reported (Huntress et al. 1991; Crovisier et al. 1991). A firm detection of carbon chain oxides in comets could also be used to support the hypothesis that the presence of O-bearing species, and in particular C₃O, in carbon stars, such as IRC+10216, is due to sublimation of orbiting icy bodies as suggested by Melnick et al. (2001).

We would like to thank F. Spinella for his technical support during laboratory experiments, and C. Contavalle and C. Nocita for their assistance during observations at Noto. This research has been financially supported by INAF and MIUR research contracts.

REFERENCES

- Baratta, G. A., Leto, G., & Palumbo, M. E. 2002, *A&A*, 384, 343
 Baratta, G. A., & Palumbo, M. E. 1998, *J. Opt. Soc. Am.* 15, 3076
 Bennett, C. J., Jamieson, C., Mebel, A. M., & Kaiser, R. I. 2004, *Phys. Chem. Chem. Phys.*, 6, 735
 Boland, W., & de Jong, T. 1982, *ApJ*, 261, 110
 Bottinelli, S., Ceccarelli, C., Williams, J. P., & Lefloch, B. 2007, *A&A*, 463, 601
 Bringa, E. M., & Johnson, R. E. 2004, *ApJ*, 603, 159
 Brown, R. D., Eastwood, F. W., Elmes, P. S., & Godfrey, P. D. 1983, *J. Am. Chem. Soc.*, 105, 6496
 Brown, R. D., et al. 1985, *ApJ*, 297, 302
 Chiar, J. E., Adamson, A. J., Kerr, T. H., & Whittet, D. C. B. 1994, *ApJ*, 426, 240
 ———. 1995, *ApJ*, 455, 234
 Chiar, J. E., et al. 1998, *ApJ*, 498, 716
 Comoretto, G., Palagi, F., & Cesaroni, R. 1990, *A&AS*, 84, 179

- Crovisier, J., Encrenaz, T., & Combes, M. 1991, *Nature*, 353, 610
- Ehrenfreund, P., Boogert, A. C. A., Gerakines, P. A., Tielens, A. G. G. M., & van Dishoeck, E. F. 1997, *A&A*, 328, 649
- Elias, J. H. 1978, *ApJ*, 224, 857
- Ford, K. E. S., Neufeld, D. A., Goldsmith, P. F., & Melnick, G. J. 2003, *ApJ*, 589, 430
- Ford, K. E. S., Neufeld, D. A., Schilke, P., & Melnick, G. J. 2004, *ApJ*, 614, 990
- Fraser, H. J., Collings, M. P., Dever, J. W., & McCoustra, M. R. S. 2004, *MNRAS*, 353, 59
- Gerakines, P. A., & Moore, M. H. 2001, *Icarus*, 154, 372
- Gerakines, P. A., Schutte, W. A., & Ehrenfreund, P. 1996, *A&A*, 312, 289
- Gerakines, P. A., et al. 1999, *ApJ*, 522, 357
- Goldsmith, P. F., & Langer, W. D. 1999, *ApJ*, 517, 209
- Guelin, M., Langer, W. D., & Wilson, R. W. 1982, *A&A*, 107, 107
- Hasegawa, T. I., & Herbst, E. 1993, *MNRAS*, 261, 83
- Hasegawa, T. I., et al. 2006, *ApJ*, 637, 791
- Huntress, W. T., Allen, M., & Delitsky, M. 1991, *Nature*, 352, 316
- Ioppolo, S., Palumbo, M. E., Baratta, G. A., & Mennella, V. 2008, *A&A*, submitted
- Kaifu, N., et al. 2004, *PASJ*, 56, 69
- Kerkhof, O., Schutte, W. A., & Ehrenfreund, P. 1999, *A&A*, 346, 990
- Kerr, T. H., Adamson, A. J., & Whittet, D. C. B. 1993, *MNRAS*, 262, 1047
- Loeffler, M. J., Baratta, G. A., Palumbo, M. E., Strazzulla, G., & Baragiola, R. 2005, *A&A*, 435, 587
- Matthews, H. E., Irvine, W. M., Friberg, P., Brown, R. D., & Godfrey, P. D. 1984, *Nature*, 310, 125
- Melnick, G. J., Neufeld, D. A., Ford, K. E. S., Hollenbach, D. J., & Ashby, M. L. N. 2001, *Nature*, 412, 160
- Mennella, V., Baratta, G. A., Esposito, A., Ferini, G., & Pendleton, Y. J. 2003, *ApJ*, 587, 727
- Mulas, G., Baratta, G. A., Palumbo, M. E., & Strazzulla, G. 1998, *A&A*, 333, 1025
- Nummelin, A., Whittet, D. C. B., Gibb, E. L., Gerakines, P. A., & Chiar, J. E. 2001, *ApJ*, 558, 185
- Ohishi, M., et al. 1991, *ApJ*, 380, L39
- Palumbo, M. E., Ferini, G., & Baratta, G. A. 2004, *Adv. Space Res.* 33, 49
- Palumbo, M. E., & Strazzulla, G. 1993, *A&A*, 269, 568
- Park, I. H., Wakelam, V., & Herbst, E. 2006, *A&A*, 449, 631
- Pontoppidan, K. M., et al. 2003, *A&A*, 408, 981
- Shuping, R. Y., Chiar, J. E., Snow, T. P., & Kerr, T. 2001, *ApJ*, 547, L161
- Strazzulla, G., Baratta, G. A., & Palumbo, M. E. 2001, *Spectrochim. Acta Astron.*, 57, 825
- Strazzulla, G., Brucato, J. R., Palumbo, M. E., & Satorre, M. A. 1997, *A&A*, 321, 618
- Strazzulla, G., & Johnson, R. 1991, in *Comets in the Post Halley Era*, ed. R. L. Newburn & M. Neugebauer (Dordrecht: Kluwer), 243
- Tegler, S. C., Weintraud, D. A., Rettig, T. W., Pendleton, Y. J., Whittet, D. C. B., & Kulesa, C. A. 1995, *ApJ*, 439, 279
- Teixeira, T. C., & Emerson, J. P. 1999, *A&A*, 351, 292
- Teixeira, T. C., Emerson, J. P., & Palumbo, M. E. 1998, *A&A*, 330, 711
- Tenenbaum, E. D., Aponi, A. J., Ziurys, L. M., Agundez, M., Cernicharo, J., Pardo, J. R., & Guelin, M. 2006, *ApJ*, 649, L17
- Tielens, A. G. G. M., & Allamandola, L. J. 1987, in *Physical Processes in Interstellar Clouds*, ed. G. E. Morfill & M. Scholer (Dordrecht: Reidel), 333
- Tielens, A. G. G. M., Tokunaga, A. T., Geballe, T. R., & Baas, F. 1991, *ApJ*, 381, 181
- Trottier, A., & Brooks, R. L. 2004, *ApJ*, 612, 1214